

14A.3 UTILIZING HETEROGENEOUS RADAR SYSTEMS IN A REAL-TIME HIGH RESOLUTION ANALYSIS AND SHORT-TERM FORECAST SYSTEM IN THE DALLAS/FORT WORTH TESTBED

Keith A. Brewster*¹, Frederick H. Carr^{1,2}, Kevin W. Thomas¹ and Derek R. Stratman²

¹Center for Analysis and Prediction of Storms

²School of Meteorology

University of Oklahoma

Norman, OK 73072

1. INTRODUCTION

The CASA Dallas/Ft. Worth Testbed (D/FW Testbed) has been established as a site for evaluating real-time observing systems, data analysis and short-term forecasting over an urban area. A number of high-density observing networks are being tested in the region, including citizen weather observations, mobile sensors, and ground based profilers. Prominent among the sensors being tested are X-band Doppler radars, including those from the Collaborative Adaptive Sensing of the Atmosphere (CASA) project (McLaughlin et. al, 2009) and from private companies, including Ridgeline, EWR, and Enterprise Electronics. The X-band radars, combined with the S-band WSR-88D (NEXRAD) radars and the C-band Terminal Doppler Weather Radars (TDWR), form a unique heterogeneous radar network that CAPS is utilizing in our real-time analysis, nowcasting and short-term numerical weather prediction (NWP) efforts.

Building on our experience from the CASA Integrated Project-1 (IP1) in Oklahoma we have configured a 3DVAR with cloud analysis system with 400-m grid spacing and an NWP system with 1-km grid spacing for 0-to-2 hour forecasts with low latency. Besides providing real-time information for local governments and the National Weather Service Forecast Office in Fort Worth, the system can be used as a basis for the testing of observation system impacts, including Networks of Networks being integrated into the National Mesonet Program. This work describes the D/FW Testbed and the current real-time analysis forecasting system.

Additionally, a unique enhancement to the Incremental Analysis Updating (IAU) data assimilation method is introduced and tested. Some recent cases of severe storms in the network during are presented as examples.

2. CASA DALLAS-FORT WORTH TESTBED

In anticipation of the CASA IP-1 X-band radars being moved to North Texas from Oklahoma as a cornerstone of the D/FW Testbed, the domain for the CAPS real-time analysis and NWP system was relocated from Oklahoma to the D/FW area in the spring of 2012. At the same time, thanks to cooperation among the NOAA Radar Operations Center, NWS Southern Region Headquarters and the NOAA National Severe Storms Lab, CAPS gained real-time access to the Level-II data from the two D/FW area C-band TDWR radars, covering the Dallas/Ft Worth International Airport (TDFW) and Dallas Love Field (TDAL).

As of September, 2015 there are five X-band radars deployed in the CASA D/FW Testbed (Fig 1), two relocated from the original CASA IP1 Network in southwestern Oklahoma, one Ridgeline Instruments radar, one EWR radar and one Enterprise Electronics (EEC) radar. There are plans for three more, including the remaining IP1 radars and a second EEC radar. These are in addition to the three Federal radars in the immediate area, namely the NEXRAD (WSR-88D) at Fort Worth (KFWS) and the two TDWR radars. The systems also utilize other more distant, NEXRAD radars that cover portions of the analysis and/or forecast domain.

*Corresponding author address: Keith Brewster,
120 David L. Boren Blvd., Suite 2500,
Norman, OK 73072, kbrewster@ou.edu

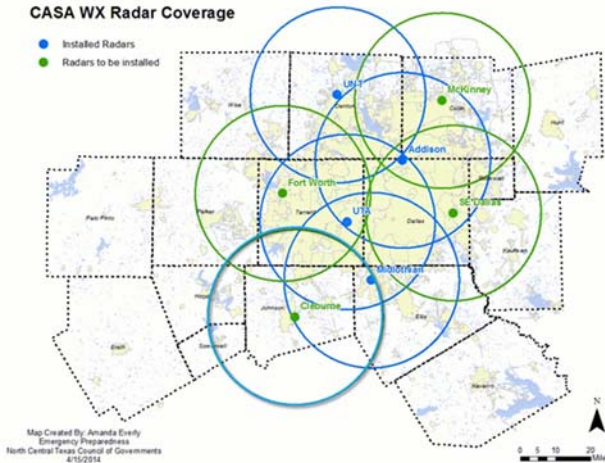


Fig. 1. Current status of CASA X-band Radar Network in Dallas-Ft. Worth Testbed. Blue circles indicate 40-km range rings for radars currently deployed. Green circles are for planned radar sites, expected to be deployed in 2015. Background map shows county boundaries of the NCTCOG

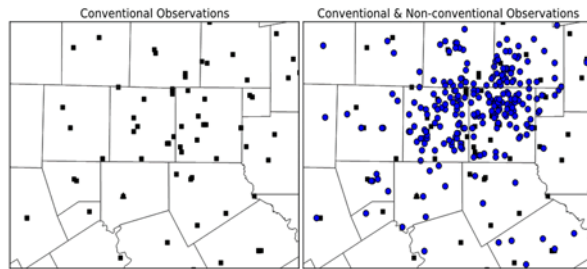


Fig. 2 Sample station location plot for surface stations in the D/FW Testbed area from 15 May 2013. Left: Conventional AWOS and ASOS sites. Right; non-conventional stations including CWOP and EarthNetworks WxBug sites

In addition to the radars and conventional observation systems, a number of additional non-conventional instruments are in the region, or will soon be brought into the testbed, as listed in Table 1. To highlight a few, the standard suite of surface observations from the National Weather Service (NWS) and Federal Aviation Administration (FAA) are augmented with additional surface observations from the EarthNetworks WeatherBug network as well as the NOAA Citizen Weather Observer Program (CWOP), e.g. Fig 2. Additionally, mobile data from commercial trucks are provided by the Mobile Platform Environmental Data (MoPED) system from GST, Inc. (Heppner, 2013). SODARs from WeatherFlow, Inc., and temporary deployments of low-level profiling units from the NSSL/OU Collaborative Lower Atmospheric Mobile Profiling System (CLAMPS) have also been used.

Table 1. Observations in Dallas-Ft Worth Testbed

Conventional Observations	Non-Conventional Observations
ASOS	EarthNetworks (WxBug)
AWOS	CWOP
West Texas Mesonet	GST MoPED
Oklahoma Mesonet	
S-band WSR-88D Radars	X-band Radars
	C-band TDWR Radars
Radiosondes	SODAR
	Radiometers

3. BUILDING THE X-BAND RADAR NETWORK

As the X-band radar network is built-out candidate sites are evaluated using principles and techniques that had been used to build the IP-1 radar network in Oklahoma (Brewster et al., 2005). The primary goals being to have broad coverage areas, significant overlap of X-band radars, good dual-Doppler crossing angles and low-level coverage to supplement NEXRAD. Logistical concerns, such as the availability of affordable power and high-speed networking, and a suitable elevated structure (such as a rooftop) free of obstructions also play a role in the siting of the radars.

Figure 3 and the first column of Table 2 show results of an analysis of the low-level coverage of the Federal radars in the D/FW Testbed. There is some dual-Doppler coverage provided by these three radars, but the alignment of the TDWR radars along nearly the same radial of the Fort Worth NEXRAD is not optimal for this purpose.

Considering the planned X-band network alone (Figure 4 and the second column of Table 2), it offers good coverage in the D/FW Testbed region with 48% of the coverage area having overlap of two

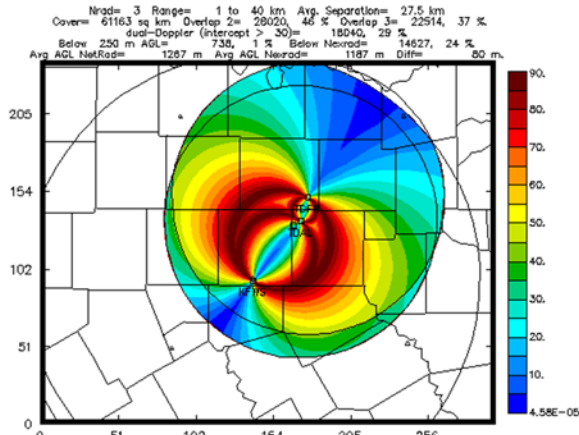


Fig. 3 Maximum dual-Doppler crossing angles (color, degrees, scale at right) for the Federal radars in the Dallas-Ft Worth Testbed, including the NEXRAD (120 km range ring) and TDWR radars (60 km range rings).

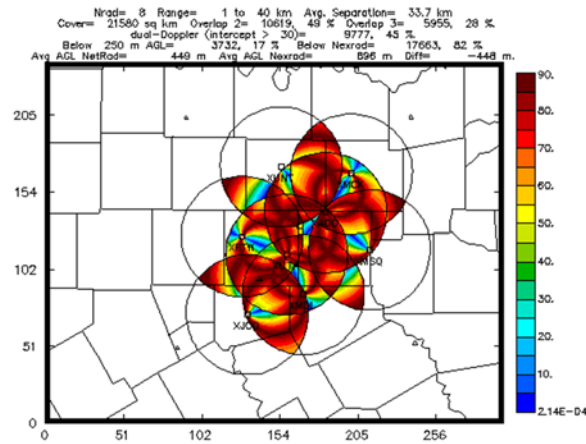


Fig. 4 Maximum dual-Doppler crossing angles (color, degrees, scale at right) for the eight planned CASA X-band radar network (40 km range rings).

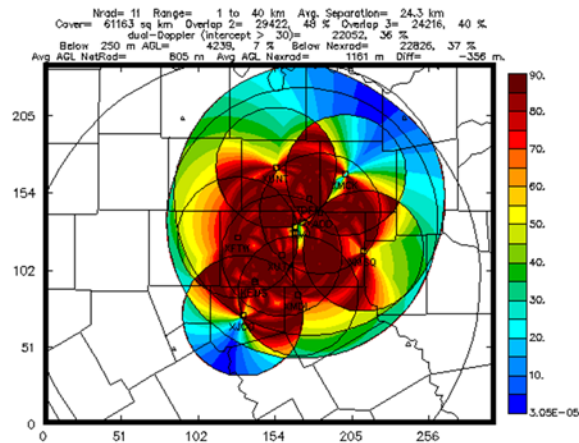


Fig. 5 Maximum dual-Doppler crossing angles (color, scale at right) for combined Federal and CASA X-band network three radars.

Table 2 Features of Radar Networks

	Federal Radars	CASA X-band	Combined
Coverage (km ²)	61 k	22 k	61 k
2-radar Overlap	46%	49%	48%
Mean Minimum Beam Height	1267 m	449 m	805 m
>30° dual Doppler	29%	45%	36%

or more radars, and 28% of the coverage area having coverage from three or more radars. 45% of the dual-Doppler area has 30° or better crossing angles allowing for excellent wind retrieval using dual-Doppler or 3DVAR methods. The mean height of the lowest beam in the X-band radar network is less than 500 m AGL. The combined radar network (Figure 5 and the third column of Table 2) has the coverage area of the Federal radar (120 km radius from KFWS was used for this analysis), but with improved minimum beam height and dual-Doppler crossing angles.

4. REAL-TIME ANALYSES AND FORECASTS DESIGN

CAPS designed a 400-m grid resolution real-time analysis and 1-km real-time data assimilation, nowcasting and numerical weather prediction system (NWP) using the Advanced Regional Prediction System (ARPS, Xue et al., 2001; Xue et al., 2003), and the ARPS 3D-Variational (3DVAR) with cloud analysis (Gao et al., 2004; Brewster et al., 2005; Hu et al. 2006a,b, Brewster et al., 2015) and ran the system in a domain covering central and southwest Oklahoma (Brewster et al., 2007 and 2010). The system as repositioned for the D/FW DFW Testbed is described below with summary details for the analysis and forecast in Tables 3 and 4, respectively.

The analysis is performed every 5 minutes on a 160x160 km grid with 400 m resolution. The focus for the analysis on tracking low-level signatures of storms and precursors for convective initiation so the top of the analysis domain is 15 km AGL, using 28 vertical levels with an average spacing of 600 m, and minimum of 20 m near the ground, first level at anemometer height (10 m AGL). The analyses are run on 192 Xeon Sandy Bridge cores of Boomer at the OU Supercomputing Center for Research and Education (OSCER).

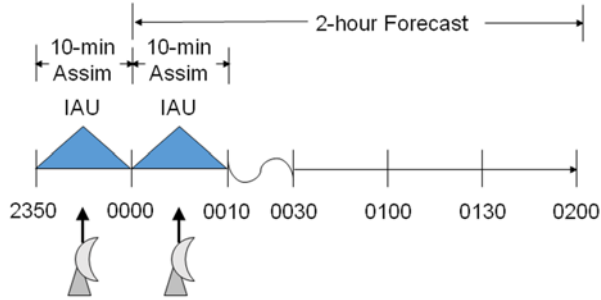


Fig. 6 Data assimilation timeline diagram for a sample 0000 UTC forecast initial time, showing observation insertion in two IAU steps as part of a 2-hour forecast

Table 3. Features of Real-Time 400-m Analyses

Method	3DVAR & Complex Cloud Analysis
Processors	192 Cores MPI
Interval	5 minutes
Typical Run Time	~6 minutes
Grid Spacing	400 m
Vertical Grid Spacing	600 m mean 20 m minimum
Grid Dimensions	448 x 456 x 28

Table 4 Features of Real-Time NWP Forecasts

Model	ARPS
Assimilation	2 cycles IAU
Processors	192 Cores MPI
Interval	15 minutes
Forecast Time	0-2 hours
Typical Run Time	20-25 minutes
Grid Spacing	1 km
Vertical Grid Spacing	400 m mean 20 m minimum
Grid Dimensions	363 x 323 x 53

The total time for the analyses, including image post processing is about 6 minutes so two sets of cores are used.

Data assimilation and short-term forecasting are run on a 353 x 320 km domain with 1-km grid spacing. 53 vertical grid levels are used with domain top at 20 km and enhanced vertical resolution near the ground (20 m minimum vertical grid spacing).

Data are assimilated by calculating the increments from the most recent 12-km NAM background forecast valid at the 10-minutes before the nominal initial time using 3DVAR, then using them in an incremental analysis updating scheme (IAU, Bloom et al., 1996) over a 10 minute period with triangular weighting. Then, a 2-hour forecast is run, including a second IAU cycle, as shown in Figure 6. The IAU allows the model to ingest the observation information, including the cloud and precipitation variables and associated latent heating, while allowing the model to come into balance by the end of the assimilation window.

For the short-term forecast there is no cumulus parameterization, clouds and precipitation are modeled using the Lin 3-Ice scheme (Lin et al., 1983). The model uses NASA Goddard atmospheric radiation transfer parameterization. Surface fluxes are calculated from stability-dependent surface drag coefficients using predicted surface temperature and volumetric water content. The model employs a simple two-layer force-store soil model based on Noilhan and Planton (1989).

The NWP model is run when there is significant precipitation in the D/FW Testbed area or when precipitation is expected and the X-band radars are running. The model is run on 192 cores of OSCER Boomer every 15 minutes. The model, including image post-processing takes about 20-25 minutes to run so two sets of cores are used.

Interested readers can find the real-time analysis and forecast products on the Web during our operational periods via the links at <http://forecast.caps.ou.edu>.

5. RECENT EXAMPLES

Two brief examples are presented from recent events in the Dallas-Ft. Worth Testbed. The first is an analysis from a case of damaging winds from a brief tornado and subsequent mesoscale convective vortex (MCV) that passed through northern Dallas County on the afternoon of 8 May 2014. On 8 May two CASA X-band radars were operational, Arlington (XUTA) and Midlothian (XMDL).

Figure 7 shows analysis output at 1-km AGL at 2030 UTC showing vertical vorticity in a developing of the MCV as the moderate squall line traversed

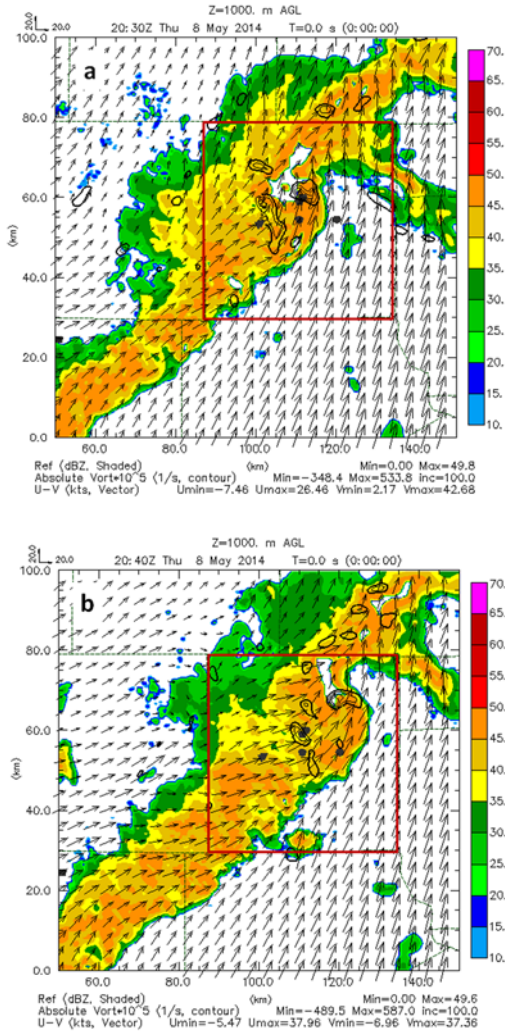


Fig. 7 Analyses 8 May 2014 at 1.0 km AGL for a) 2030 and b) 2040 UTC. Reflectivity (dBZ) in color, wind vectors and vertical vorticity $> 100 \times 10^{-5} \text{ sec}^{-1}$ contours.

northern Dallas Co. (highlighted with red boundary). The analysis shows an area of rotation in in central Dallas Co. at 2030 UTC that had progressed from southwest to northeast through the northern half of the county, exiting at the northeast corner at 2050 UTC

Regarding the forecasts, we examine a sequence of forecasts produced during a severe weather outbreak on the afternoon of 2 Oct 2014. Two CASA radars were operational on that day, at Arlington and Midlothian. Severe weather in Texas on 2 Oct 2014 was associated with a squall line that formed in, and just west of, the D/FW Testbed and propagated eastward during the late afternoon.

We examine here the forecasts and verification data valid at 2100 UTC, considering forecasts

initialized from 1900 UTC to 2030 UTC (actual forecast interval was 15-min, every-other one is shown here for clarity). Looking at this sequence one can see how the forecast for that time evolved with successive forecasts.

The forecast initialized at 1900 UTC had good skill in predicting the development and propagation of the squall line from Dallas-Ft. Worth and northward, while missing the development of the tail of the squall line further south. The 1930 UTC forecast did a better job, and then by the 2000 UTC forecast the southward extent of the line was reasonably well forecasted. The forecasts include an enhanced bulge on the line that is seen in the verification toward the south end of the line.

Some other verification times and an examination of the winds from this case are presented in Brewster et al., 2014.

6. IAU WITH VARIABLE-DEPENDENT TIMING

Examining the vertical cross sections in this and other cases of strong thunderstorms and/or squall lines in the initial conditions revealed some difficulties in establishing an updraft in a strong convective storm from a larger-scale background without such a storm. There was some evidence in the first IAU cycle of difficulty in maintaining the observed hail/graupel maxima. In our current real-time system, the increments for all variables are applied using the same triangular distribution with the largest share of the increments applied in the middle of the time window (as indicated in Fig 6).

It may be possible to improve the support of the weight of the hail, graupel and heavy rain by first adjusting the wind and mass fields to allow the updraft velocities to become established without significant rain and hail loading, and possible decelerating cooling due to melting of falling hail and/or graupel. This can be accomplished by adjusting the increment distribution in time so that a larger fraction of the latent heat and wind increments are applied early in the IAU window, and also introducing the hydrometeors using a different time weighting that applies most of those increments toward the end of the IAU window. We term this IAU with Variable Dependent Timing (IAU-VDT).

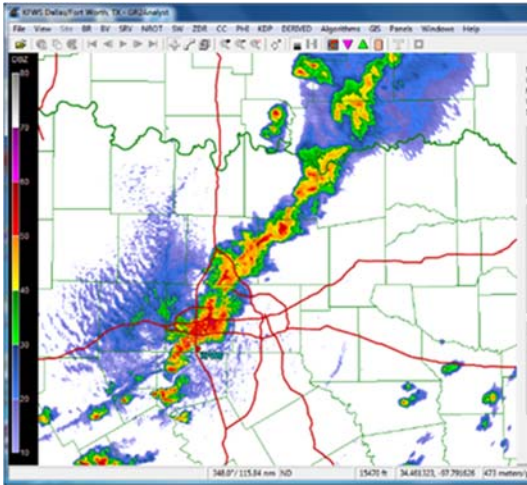


Fig. 8 Verifying 0.5 degree KFWS at 2100 UTC, radar reflectivity (dBZ, color scale at left)

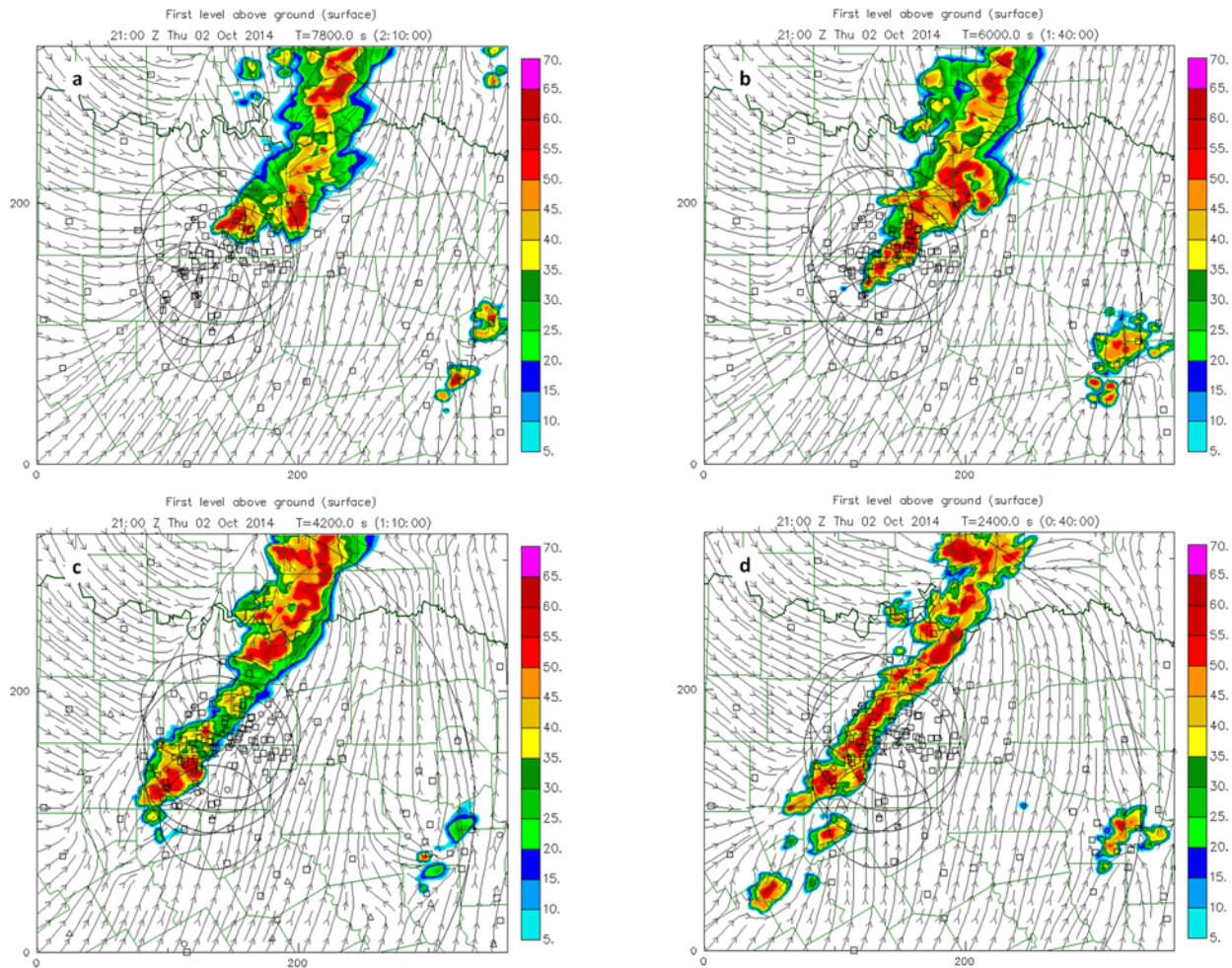


Fig. 9 Forecast results valid at 2 Oct 2014 2100 UTC from four forecasts with initial times: a) 1900, b) 1930, c) 2000, d) 2030 UTC. Simulated reflectivity at first model level (20 m AGL) and surface streamlines

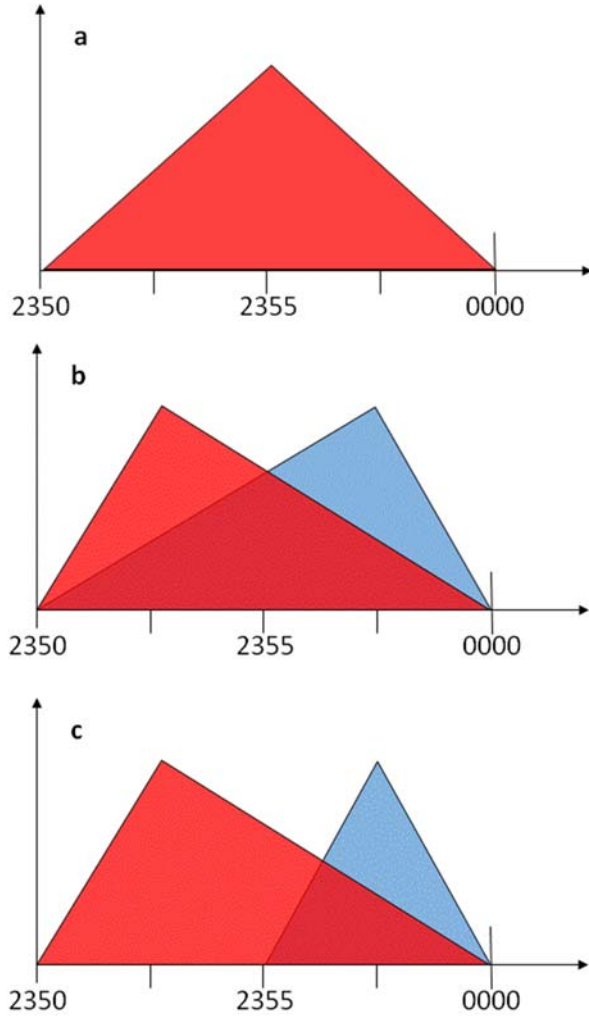


Fig. 10 Three IAU-VDT time weighting shape pairs: a) A: Uniform triangular weighting b) B: early mass-wind bias (red) with late hydrometeor bias (blue) c) C: early mass-wind bias (red) with delayed-start hydrometeor insertion (blue).

The ARPS IAU code was modified to allow user specification of the IAU increment weighting in more than one shape, and assign a shape for each variable, then apply these shapes during the IAU window. To test the IAU-VDT we define three shape couples, the centered triangular shape uniformly applied to all variables as is used in common IAU systems (Shape A, Fig 11a), a triangular weighting that is biased toward the beginning of the assimilation window for mass and wind fields with a triangular weighting biased toward the end of the assimilation window (Shape B, Fig. 11b) and a weighting for mass and wind as in Shape B, but with no hydrometeor insertion until the middle of the assimilation window (Shape C, Fig11c). The test case will be 24 April 2015, a case of a strong squall

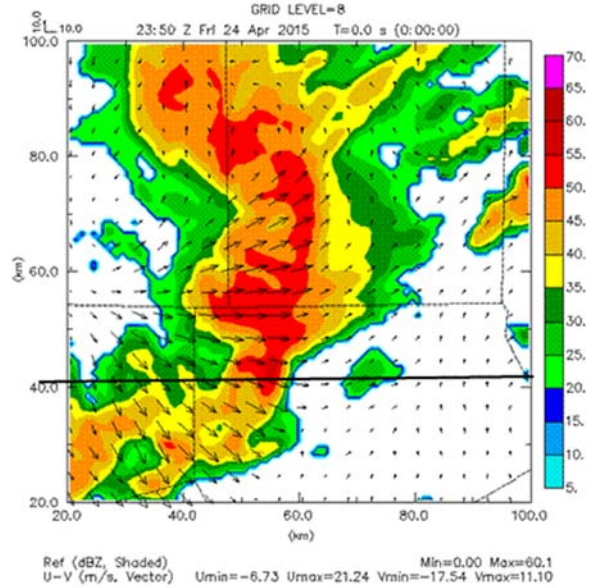


Fig. 11 Initial reflectivity (dBZ, colors) and wind at grid level 8 at 2350 UTC (using mosaicked data from 2350-UTC) that is used to generate analysis increments for IAU in the 2350-0000 assimilation window. Cross-sections along $y=40.5$ km as indicated by horizontal line.

line passing through the CASA DFW Testbed with wind high winds and hail observed (Fig 12). We will examine east-west vertical cross-sections as along $y=40.5$ km as indicated by horizontal line in Fig 12.

Figure 13 shows the hydrometeor estimates from the cloud analysis using the Milbrant and Yau single-moment microphysics (Milbrant and Yau, 2005a, 2005b). A hail and graupel core is analyzed with maxima as indicated in the first column of Table 5.

Figure 14 shows the result of the 10-minute forecast/assimilation with the analysis increments applied using the three IAU-VDT schema previously described. The maxima after the assimilation are recorded in columns 2-4 of Table 5. It is apparent from the Figures that there is improvement in retention of updraft vertical velocity, hail and graupel using Scheme B over the traditional equally-weighted Scheme A, particularly in the hail core between 3 and 6 km. There is additional improvement when delaying the start of hydrometeor assimilation as shown in the results for Scheme C, again in the hail core aloft as well as in the maximum values of graupel and hail. There is also apparent improvement in the structure of the hail core, being less spread out horizontally in the lowest 3 km, after applying Scheme C compared to the other IAU shapes

Table 5 Maxima of Selected Variables after first IAU time window (2350-0000 UTC)

Variable	Analysis	IAU-Orig	IAU-B	IAU-C
Rain	5.3 g/kg	2.4	2.7	3.3
Snow	14.3 g/kg	4.0	5.3	10.0
Graupel	6.0 g/kg	2.1	2.1	2.0
Hail	2.0 g/kg	0.3	0.3	0.6
W	8.4 m/s	6.2	7.5	7.9

7. SUMMARY AND FUTURE WORK

A real-time high-resolution data analysis and short-term NWP system has been set-up for the D/FW Testbed. At the time of publication five X-band radars have been sited, and locations for additional X-band radars have been identified considering needs for dual-Doppler analysis, low-level coverage and deployment logistics. The X-band radar network is expected to be complete by spring 2016. Once the radar network is complete, formal quantitative evaluation will be done of precipitation forecasts using Equitable Threat Scores and object-based methods for tornadoes, following recent work of Stratman and Brewster, 2015. Separately, training of forecasters and emergency managers in the use of these and other CASA tools will begin in early 2016, with subjective evaluation by stakeholders to follow, based on results.

The complex cloud analysis system is being updated and will include hydrometeor assignment specific to each available microphysics option, including the multi-moment schemes. This will allow better initialization of microphysics options other than Lin 3-ice. Use of a 2-moment Milbrandt and Yau scheme is planned for the real-time system after an OSCER computer upgrade this fall.

One objective of the D/FW Testbed, as part of the National Mesonet effort, is to identify the impact of the novel observation systems on the analyses and forecasts. This will be carried-out via OSSEs, data denial experiments and evaluation of analysis sensitivity to each data source.

A unique enhancement to the IAU assimilation scheme has been developed and demonstrated, IAU with Variable Dependent Timing, IAU-VDT. Further testing of different VDT shapes is planned with operational implementation to follow shortly.

8. ACKNOWLEDGMENTS

The D/FW Testbed and CASA work is supported in part by the National Science Foundation (NSF) under EEC03-13747, by the NWS, and the North Central Texas Council of Governments. Brenda Philips and Apoorva Bajaj of the University of Massachusetts lead the D/FW CASA X-band Testbed activities.

The authors would like to thank ROC staff, particularly Tim Crum, and Karen Cooper of NSSL for their help in gaining access to the real-time Level-II TDWR data for the D/FW Testbed.

Oklahoma Mesonet data provided by the Oklahoma Climatological Survey. West Texas Mesonet data provided by Texas Tech University.

Supercomputing resources from the Oklahoma University Supercomputer Center for Education and Research (OSCER) were used for the analyses and forecasts in this study.

Any opinions, findings, conclusions, or recommendations expressed in this material are those of the authors and do not necessarily reflect those of the funding agencies nor the host universities.

9. REFERENCES

- Bloom, S. C., L. L. Takacs, A. M. da Silva, D. Ledvina, 1996: Data Assimilation Using Incremental Analysis Updates. *Mon. Wea. Rev.*, **124**, 1256–1271.
- Brewster, K.A. F.H. Carr, K.W. Thomas and D.R. Stratman, 2015: Utilizing heterogeneous radar systems in a real-time high resolution analysis and short-term forecast system in the Dallas/Ft. Worth Testbed. *Preprints, 37th Conference on Radar Meteorology*, Amer. Meteor. Soc., Paper 31.
- Brewster, K., M. Hu, M. Xue, and J. Gao, 2005: Efficient assimilation of radar data at high resolution for short range numerical weather prediction. World Weather Research Program Symposium and Nowcasting and Very Short-Range Forecasting WSN05, Toulouse, France. WMO World Weather Research Program, Geneva, Switzerland. Symposium CD, Paper 3.06.
- Brewster, K.A. and D.R. Stratman, 2015: An updated high-resolution hydrometeor analysis system using radar and other data. *Preprints, 27th Conference on Wea. Analysis and*

- Forecasting and 23rd Conf. on Numerical. Wea. Pred.*, Amer. Meteor. Soc., Paper 31.
- Brewster, K.A., K. W. Thomas, J. Brotzge, Y. Wang, D. Weber, and M. Xue, 2007: High resolution assimilation of CASA X-band and NEXRAD radar data for thunderstorm forecasting. 22nd Conf. Wea. Anal. Forecasting/18th Conf. Num. Wea. Pred., Salt Lake City, Utah, Amer. Meteor. Soc., Paper 1B.1
- Brewster, K., K.W. Thomas, J. Gao, J. Brotzge, M. Xue, and Y. Wang, 2010: A nowcasting system using full physics numerical weather prediction initialized with CASA and NEXRAD radar data. Preprints, 25th Conf. Severe Local Storms, Denver, CO, Amer. Meteor. Soc., Denver, CO, Paper 9.4.
- Brewster, K., L. White, B. Johnson, and J. Brotzge, 2005: Selecting the sites for CASA NetRad, a collaborative radar network. Ninth Symposium on Integrated Observing and Assimilation Systems for the Atmosphere, Oceans and Land Surface (IOAS-AOLS), 85th Amer. Meteor. Soc. Annual Meeting CD, Paper: P3.4.
- Gao, J., M. Xue, K. Brewster, and K. K. Droegemeier 2004: A three-dimensional variational data assimilation method with recursive filter for single-Doppler radar, *J. Atmos. Oceanic. Technol.* 457-469.
- Heppler, P.O.G, 2013, Building a National Network of Mobile Platforms for Weather Detection, 29th Conf. on Environ. Information Processing Technologies, Amer. Meteor. Soc., Recorded presentation:
https://ams.confex.com/ams/93Annual/recordin_gredirect.cgi/id/23230
- Hu, M., M. Xue, and K. Brewster, 2006a: 3DVAR and cloud analysis with WSR-88D Level-II Data for the Prediction of Fort Worth Tornadoic Thunderstorms Part I: Cloud analysis and its impact. *Mon. Wea. Rev.*, **134**, 675-698.
- Hu, M., M. Xue, J. Gao and K. Brewster: 2006b: 3DVAR and Cloud Analysis with WSR-88D Level-II Data for the Prediction of Fort Worth Tornadoic Thunderstorms Part II: Impact of radial velocity analysis via 3DVAR, *Mon Wea Rev.*, **134**, 699-721.
- Milbrandt, J. A. and M. K. Yau, 2005a: A Multimoment Bulk Microphysics Parameterization. Part I: Analysis of the Role of the Spectral Shape Parameter. *J. Atmos. Sci.*, **62**, 3051–3064.
- Milbrandt, J. A. and M. K. Yau, 2005b: A Multimoment Bulk Microphysics Parameterization. Part II: A Proposed Three-Moment Closure and Scheme Description. *J. Atmos. Sci.*, **62**, 3065–3081.
- National Research Council, 2009, *Observing Weather and Climate from the Ground Up. A Nationwide Network of Networks*. The National Academies Press, Wash. DC, 250 pp.
<http://books.nap.edu/catalog/12540/>
- Noilhan, J. and S. Planton, 1989: A simple parameterization of land surface processes for meteorological models. *Mon. Wea. Rev.*, **117**, 536-549.
- Stratman, D. and K. Brewster, 2014, Comparison of 24 May 2011 genesis and evolution of simulated mesocyclones using various microphysics schemes with 1-km resolution. 27th Conf. Severe Local Storms, Amer. Meteor. Soc., Paper 54.
- Sun, W.-Y., and C.-Z. Chang, 1986: Diffusion model for a convective layer. Part I: numerical 864 simulation of convective boundary layer. *J. Climate App. Meteorol.*, **25**, 1445–1453.
- Xue, M., K. K. Droegemeier, V. Wong, A. Shapiro, K. Brewster, F. Carr, D. Weber, Y. Liu, and D.-H. Wang, 2001: The Advanced Regional Prediction System (ARPS) - A multiscale nonhydrostatic atmospheric simulation and prediction tool. Part II: Model physics and applications. *Meteor. Atmos. Physics*, **76**, 143-165.
- Xue, M., D.-H. Wang, J. Gao, K. Brewster, and K.K. Droegemeier, 2003: The Advanced Regional Prediction System (ARPS) – storm-scale numerical weather prediction and data assimilation. *Meteor. Atmos. Physics*, **82**, 139-170.

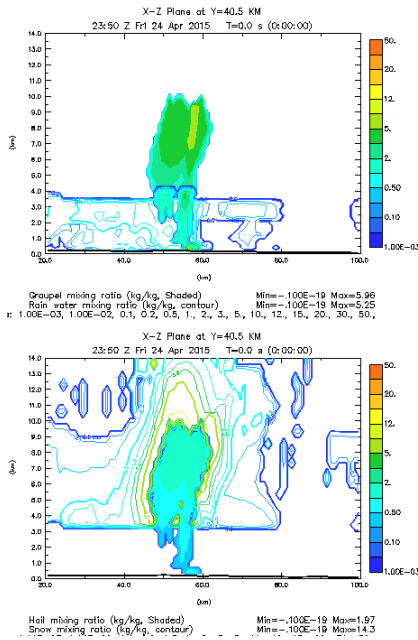


Fig. 12 East-west cross-section at $y=40.5$ km. Estimated hydrometeor fields from the complex cloud analysis at 2350 UT. Top panel: graupel (color) and rain (colored contour lines), Bottom panel: hail (color shading) and snow (color contours).

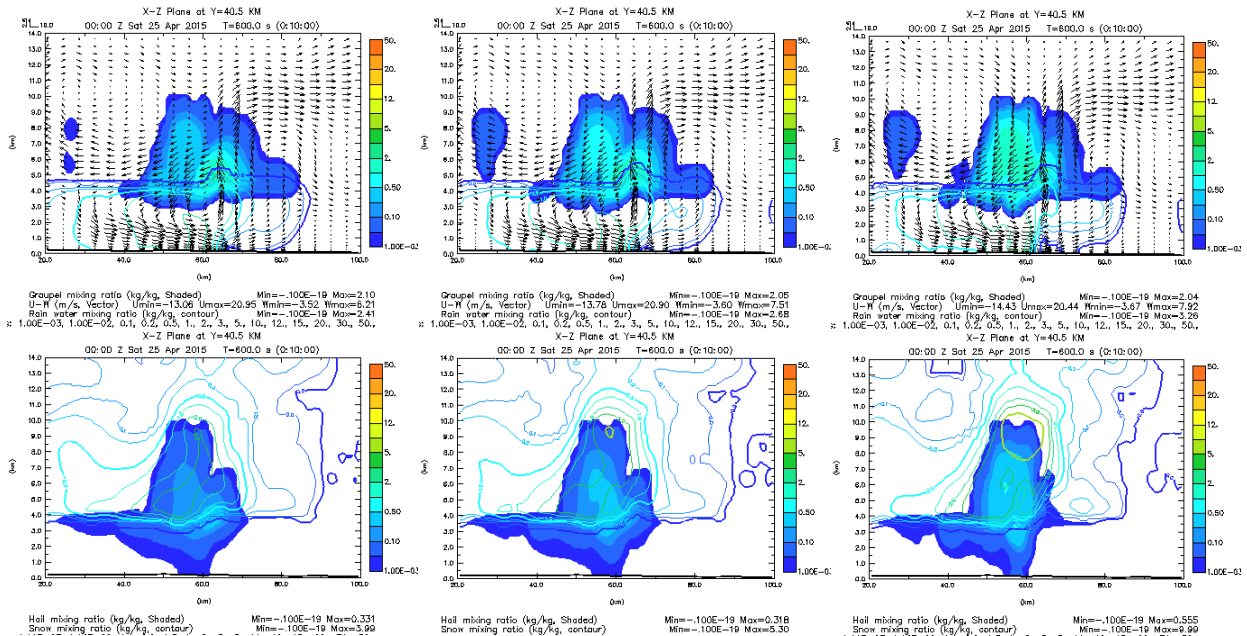


Fig. 13 Cross-section at 40.5 km after IAU assimilation window. Variables as in Fig 12. Left IAU-VDT time weighting scheme A, Center: IAU-VDT scheme B, Right: IAU-VDT scheme C.